Theoretical Assessment of New Molecules for Second-Order Nonlinear Optics

SOFIANE NOUAR LABIDI,[1,2] MOHAMMED BENALI KANOUN,[1] MARC DE WERGIFOSSE,[1] BENOÎT CHAMPAGNE[1]

[1]*Laboratoire de Chimie Théorique (LCT), Facultés Universitaires Notre-Dame de la Paix (FUNDP), Rue de Bruxelles 61, BE-5000 Namur, Belgium*

[2]*Département de Chimie, Faculté des Sciences, Centre Universitaire de Tamanrasset, Tamanrasset 11000, Algérie*

Received 30 January 2010; accepted 24 March 2010
Published online 31 August 2010 in Wiley Online Library (wileyonlinelibrary.com).
DOI 10.1002/qua.22757

ABSTRACT: The polarizabilities and first hyperpolarizabilities of nine recently synthesized compounds have been calculated ab initio to assess the effects of basis sets, of electron correlation (at the MP2 level), of frequency dispersion, and of the solvent within the polarizable continuum model, as well as to address structure–property relationships. These calculations confirm that moderate-size basis sets like 6-31+G* or 6-311+G* are enough to provide accurate estimates of the polarizabilities and first hyperpolarizabilities for these systems build from the combination of π-conjugated linkers with donor/acceptor moieties. They describe the specific behavior of the hyper-Rayleigh scattering (HRS) first hyperpolarizability and of its depolarization ratio as a function of the incident light frequency. Then, these calculations exemplify the large impact of including electron correlation and solvent effects on the first hyperpolarizabilities, and the crucial issue in view of optimizing the NLO compounds, that these effects are strongly system dependent. Finally, this theoretical investigation draws attention to the interplay between several second-order nonlinear optical molecular responses: the norm of the first hyperpolarizability (β), the projection on the dipole moment ($\beta_{//}$), which can be obtained from electric field–induced second-harmonic generation measurements, and the HRS response (β_{HRS}). Int J Quantum Chem 111: 1583–1595, 2011

Correspondence to: B. Champagne; e-mail: benoit.champagne@fundp.ac.be

Contract grant sponsors: Facultés Universitaires Notre-Dame de la Paix (FUNDP) (CERUNA Postdoctoral Grant), F.R.S.-FRFC.
Contract grant sponsor: Loterie Nationale.
Contract grant number: 2.4.617.07.F.

Additional Supporting Information may be found in the online version of this article.

Key words: first hyperpolarizabilities; HRS and EFISHG; D/A pi-conjugated systems; electron correlation and dispersion effects; solvent effects

1. Introduction

Organic compounds have gained large interest for a wide spectrum of second-order nonlinear optical (NLO) applications, ranging from electrooptical high-speed modulation for telecommunications to optical frequency conversion including terahertz generation. The advantages of these materials when compared with their inorganic counterparts are their superior optical nonlinearities, the fast electronic response, and the low dielectric constant at optical and radio frequencies [1–3].

Nevertheless, progresses to enhance the NLO properties by designing new compounds are still expected, and they rely on a multidisciplinary approach combining synthesis with experimental and theoretical characterizations [4–6]. Before addressing the properties of the bulk material, the first step consists in optimizing the molecular responses by finding appropriate interplay between the length and shape of the conjugated segment and the strengths and positions of the donor (D)/acceptor (A) groups [7–9]. Among the recent propositions of such molecular structures, some are based on porphyrin [10], fullerene and nanotube [11], and helicene [6] units as well as on extended linear π-conjugated structures with many D/A substituents [12]. The other step aims at translating large molecular responses into large second-order NLO susceptibilities and involves mastering the intermolecular interactions to induce proper ordering of the chromophores and electrostatic interactions.

In this contribution, we tackle the molecular responses in a series of nine compounds (Scheme 1) that have been recently proposed in view of achieving large second-order NLO responses. Because of their D-π-A structure, these compounds satisfy the usual criterion of high asymmetry to achieve a large first hyperpolarizability. Characterizing their responses at the molecular level and particularly in solutions constitutes the first step toward realizing large responses. Indeed, because of crystal packing and intermolecular interactions, there might be large differences between the second-order NLO responses at the molecular and crystal levels. Moreover, these investigations provide a basis for further experimental characterizations of the molecular properties in solution. The list of selected species encompasses 2-carboxylic acid-4-nitropyridine-1-oxide (POA) [13], 4-nitro-4-methyl benzylideneaniline (NMBA) [14], *N*,*N*-dimethylamino-*N*′-methylstilbazolium *p*-toluenesulfonate (DAST) [15], 4-(2,4-dichlorobenzylideneamino) antipyrine (2,4-DCBAP) and 4-(2,6-dichlorobenzylideneamino) antipyrine (2,6-DCBAP) [16], 2,4-dihydroxybenzaldehyde-4-nitrophenylhydrazone (2,4-DHNPH) and 3,4-dihydroxybenzaldehyde-4-nitrophenylhydrazone (3,4-DHNPH) [17] as well as two compounds with a strong acceptor group, 2-{3-cyano-4-[3-(1-decyl-1,4-dihydroquinolin-4-ylidene)prop-1-enyl]-5,5-dimethyl-2,5-dihydrofuran-2-ylidene}-malononitrile (CYPRM) and 2-{3-cyano-4-[5-(1-decyl-1,4-dihydroquinolin-4-ylidene)penta-1,3-dienyl]-5,5-dimethyl-2,5-dihydrofuran-2-ylidene}malononitrile (CYPEDM) [18].

Therefore, we address here the molecular properties of these new molecules by means of ab initio calculations. In particular, we focus on the first hyperpolarizability (β) as well as on the linear response, the polarizability (α). This article is dedicated to Sylvio Canuto, who has contributed significantly to this field of predicting and interpreting molecular properties by including the effects of the electron correlation [19] as well as of the solvent [20]. The next section is devoted to a brief presentation of the computational methods and of the quantities of interest, the first hyperpolarizabilities that can be measured using the hyper-Rayleigh scattering (HRS) and electric field–induced second-harmonic generation (EFISHG) techniques. Section 3 presents the results, starting with an investigation of the basis set effects, a description of the frequency dispersion for selected systems as well as of the electron correlation effects. Then, we investigate the effects of the solvent, a topic in close connection with the honored scientist. Finally, we discuss structure–property relationships. Conclusions and outlook are given in Section 4.

2. Theoretical and Computational Aspects

The molecular structures were optimized at the density functional theory level using the B3LYP exchange-correlation functional and the 6-311G* basis set (see Supporting Information). The polarizabilities

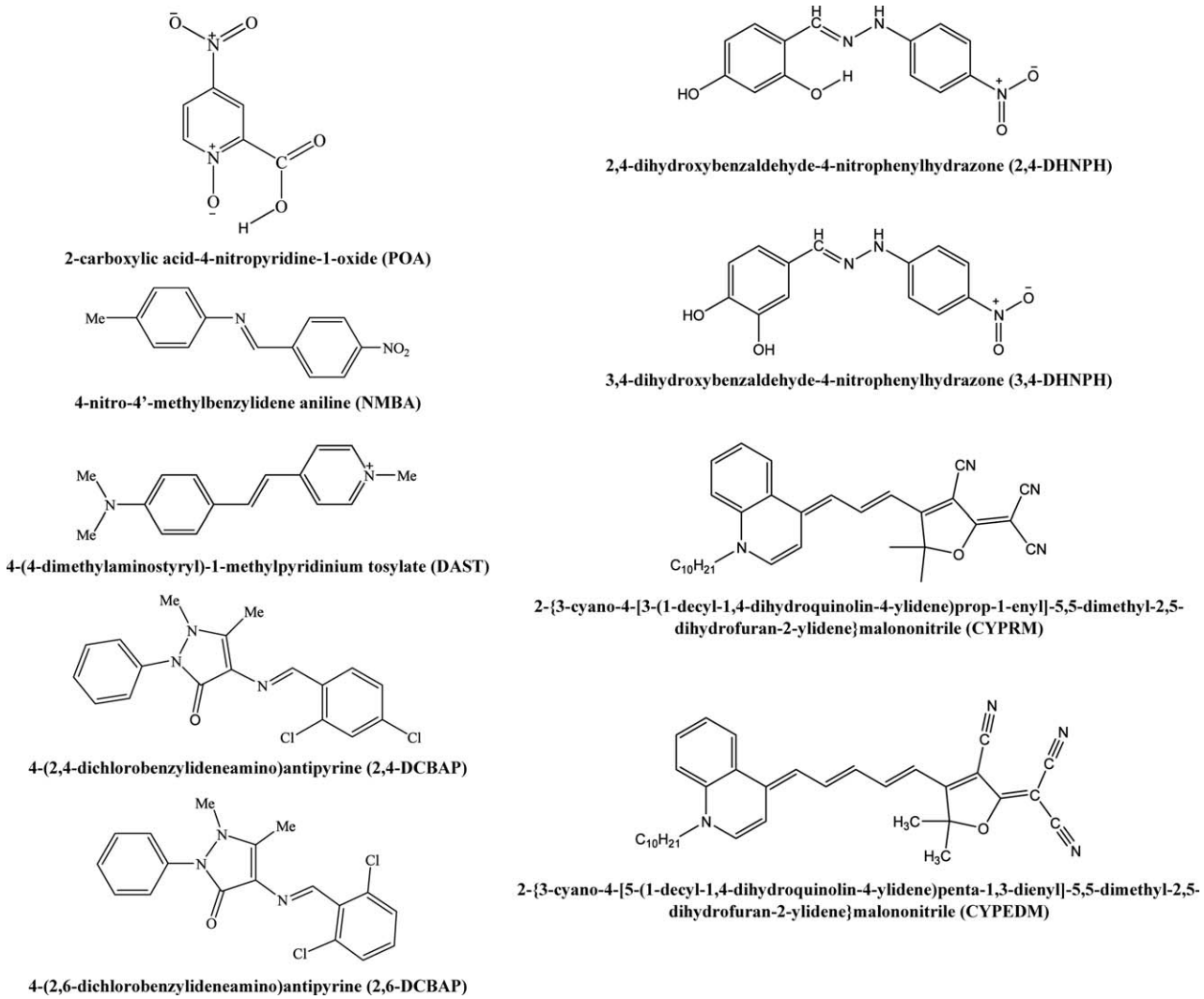

SCHEME 1. Chemical structures of the NLO compounds.

and first hyperpolarizabilities were evaluated at different levels of approximation. First, the time-dependent Hartree-Fock (TDHF) [21] and coupled perturbed Hartree-Fock (CPHF) schemes were applied for obtaining dynamic and static response properties, respectively. These methods consist in expanding the matrices of the TDHF/CPHF equations in the Taylor series of the external (static or dynamic) electric field and in solving these analytically order by order. However, taking advantage of the $2n + 1$ rule, only the first-order derivatives of the orbitals are needed to evaluate both the first-order α and the second-order β responses. The TDHF calculations were carried out using the typical wavelength (λ) of 1064 nm. To take into account the solvent effects, the polarizable continuum model within the integral equation formalism (IEF-PCM) [22] was used.

To account for correlation effects, the second-order Møller-Plesset level (MP2) method was adopted in combination with the finite field procedure. To remove higher order contaminations in the finite differentiation procedure, the Romberg method was applied [8]. Then, to account for frequency dispersion at the MP2 level, we used the multiplicative approximation, which consists in multiplying the static MP2 value by the ratio between the TDHF and CPHF values. In the case of β, this expression reads:

$$\beta_{\mathrm{MP2}}(-2\omega;\omega,\omega) \approx \beta_{\mathrm{MP2}}(0;0,0) \times \frac{\beta_{\mathrm{TDHF}}\ (-2\omega;\omega,\omega)}{\beta_{\mathrm{CPHF}}\ (0;0,0)}. \qquad (1)$$

This approximation, which assumes that frequency dispersion is the same at both the HF and correlated MP2 levels, has been shown to be a satisfactory approximation for different systems [23].

For α, we focus on the isotropic average,

$$\overline{\alpha} = \frac{1}{3}(\alpha_{xx} + \alpha_{yy} + \alpha_{zz}), \tag{2}$$

whereas for β, we consider two measurable second-order NLO responses: the HRS response and the EFISHG response. In the case of plane-polarized incident light and observation made perpendicular to the propagation plane without polarization analysis of the scattered beam, the second-order NLO response that can be extracted from HRS data reads [24]:

$$\beta_{\mathrm{HRS}} = \sqrt{\langle \beta^2_{ZZZ} \rangle (1 + 1/\mathrm{DR})}, \tag{3}$$

where DR is the depolarization ratio. The value of the depolarization ratio is mostly governed by the geometry of the NLOphore, the part of the molecule responsible for the NLO response (for an ideal D/A 1D system DR = 5, for an octupolar molecule, DR = 1.5, whereas for a Λ-shape molecule, the amplitude of DR depends on the angle between the chromophore as well as on the strengths of the D/A groups) [25].

$$\mathrm{DR} = \frac{\langle \beta^2_{ZZZ} \rangle}{\langle \beta^2_{XZZ} \rangle}, \tag{4}$$

where $\langle \beta^2_{ZZZ} \rangle$ and $\langle \beta^2_{XZZ} \rangle$ correspond to the orientational averages of the β tensor, which, without assuming Kleinman's conditions, read:

$$\begin{aligned}\langle \beta^2_{ZZZ} \rangle = {} & \frac{1}{7}\sum_{\zeta}^{x,y,z} \beta^2_{\zeta\zeta\zeta} + \frac{4}{35}\sum_{\zeta\neq\eta}^{x,y,z} \beta^2_{\zeta\zeta\eta} + \frac{2}{35}\sum_{\zeta\neq\eta}^{x,y,z} \beta_{\zeta\zeta\zeta}\beta_{\zeta\eta\eta} \\ & + \frac{4}{35}\sum_{\zeta\neq\eta}^{x,y,z} \beta_{\eta\zeta\zeta}\beta_{\zeta\zeta\eta} + \frac{4}{35}\sum_{\zeta\neq\eta}^{x,y,z} \beta_{\zeta\zeta\zeta}\beta_{\eta\eta\zeta} + \frac{1}{35}\sum_{\zeta\neq\eta}^{x,y,z} \beta^2_{\eta\zeta\zeta} \\ & + \frac{4}{105}\sum_{\zeta\neq\eta\neq\xi}^{x,y,z} \beta_{\zeta\zeta\eta}\beta_{\eta\xi\xi} + \frac{1}{105}\sum_{\zeta\neq\eta\neq\xi}^{x,y,z} \beta_{\eta\zeta\zeta}\beta_{\eta\xi\xi} \\ & + \frac{4}{105}\sum_{\zeta\neq\eta\neq\xi}^{x,y,z} \beta_{\zeta\zeta\eta}\beta_{\xi\xi\eta} + \frac{2}{105}\sum_{\zeta\neq\eta\neq\xi}^{x,y,z} \beta^2_{\zeta\eta\xi} \\ & + \frac{4}{105}\sum_{\zeta\neq\eta\neq\xi}^{x,y,z} \beta_{\zeta\eta\xi}\beta_{\eta\xi\xi} \end{aligned} \tag{5}$$

$$\begin{aligned}\langle \beta^2_{XZZ} \rangle = {} & \frac{1}{35}\sum_{\zeta}^{x,y,z} \beta^2_{\zeta\zeta\zeta} + \frac{4}{105}\sum_{\zeta\neq\eta}^{x,y,z} \beta_{\zeta\zeta\zeta}\beta_{\zeta\eta\eta} \\ & - \frac{2}{35}\sum_{\zeta\neq\eta}^{x,y,z} \beta_{\zeta\zeta\zeta}\beta_{\eta\eta\zeta} + \frac{8}{105}\sum_{\zeta\neq\eta}^{x,y,z} \beta^2_{\zeta\zeta\eta} + \frac{3}{35}\sum_{\zeta\neq\eta}^{x,y,z} \beta^2_{\zeta\eta\eta} \\ & - \frac{2}{35}\sum_{\zeta\neq\eta}^{x,y,z} \beta_{\zeta\zeta\eta}\beta_{\eta\zeta\zeta} + \frac{1}{35}\sum_{\zeta\neq\eta\neq\xi}^{x,y,z} \beta_{\zeta\eta\eta}\beta_{\zeta\xi\xi} \\ & - \frac{2}{105}\sum_{\zeta\neq\eta\neq\xi}^{x,y,z} \beta_{\zeta\zeta\xi}\beta_{\eta\eta\xi} - \frac{2}{105}\sum_{\zeta\neq\eta\neq\xi}^{x,y,z} \beta_{\zeta\zeta\eta}\beta_{\eta\xi\xi} \\ & + \frac{2}{35}\sum_{\zeta\neq\eta\neq\xi}^{x,y,z} \beta^2_{\zeta\eta\xi} - \frac{2}{105}\sum_{\zeta\neq\eta\neq\xi}^{x,y,z} \beta_{\zeta\eta\xi}\beta_{\eta\zeta\xi}. \end{aligned} \tag{6}$$

On the other hand, the EFISHG measurements give information on the projection of the vector part of β on the dipole moment vector:

$$\begin{aligned}\beta_{||}(-2\omega;\omega,\omega) = \beta_{||} &= \frac{3}{5}\sum_{\zeta}^{x,y,z} \frac{\mu_\zeta}{||\mu||}\sum_{\eta}^{x,y,z}(\beta_{\zeta\eta\eta} + \beta_{\eta\zeta\eta} + \beta_{\eta\eta\zeta}) \\ &= \frac{3}{5}\sum_{\zeta}^{x,y,z} \frac{\mu_\zeta\beta_\zeta}{||\mu||} = \frac{3}{5}||\mu||\,||\beta||\cos\theta, \end{aligned} \tag{7}$$

where $\|\mu\|$ is the norm of the dipole moment. μ and β_i are the Cartesian components of the μ and β vectors. To define β, the Taylor series expansion of the dipole moment as a function of the electric field was considered. More information on these techniques can be found in Refs. [24] and [26]. The ab initio calculations were performed using the Gaussian 03 quantum chemistry package [27], whereas the Romberg scheme was applied using a homemade code.

3. Results

3.1. BASIS SET EFFECTS

In a first step, the choice of atomic orbital basis set for determining the molecular polarizabilities and first hyperpolarizabilities was addressed by considering POA and NMBA as test compounds (Tables I and II). A difference of about 5% is obtained for the average polarizability of POA when performing the calculations with the 6-31+G* basis set in comparison with the reference aug-cc-pVTZ basis set. This difference increases to

TABLE I

Basis set effects on the TDHF (λ = 1064 nm) polarizabilities ($\bar{\alpha}$), first hyperpolarizabilities (β_{HRS}), and depolarization ratios (DR) of POA and NMBA.

	POA			NMBA		
	$\bar{\alpha}$	β_{HRS}	DR	$\bar{\alpha}$	β_{HRS}	DR
6-31G	85.65	369.8	3.37	175.45	1462.8	4.47
6-31G*	88.53	330.1	3.36	179.39	1407.5	4.53
6-31G**	88.78	329.5	3.37	180.42	1409.9	4.53
6-31+G	97.84	412.1	3.28	197.30	1634.8	4.38
6-31+G*	100.30	373.0	3.28	201.27	1587.5	4.44
6-311G*	91.28	345.5	3.34	187.84	1472.4	4.47
6-311G**	91.71	347.9	3.35	189.01	1471.1	4.47
6-311+G*	100.55	383.2	3.28	202.72	1651.3	4.45
6-311+G**	100.92	386.0	3.29	203.81	1650.1	4.45
cc-pVDZ	89.48	333.0	3.35	185.49	1422.2	4.48
cc-pVTZ	98.50	345.9	3.33	199.96	1530.7	4.50
aug-cc-pVDZ	106.05	366.9	3.33	211.76	1661.1	4.49
aug-cc-pVTZ	106.50	368.1	3.33	—	—	—

The $\bar{\alpha}$ and β_{HRS} values are given in atomic units (a.u.).

about 15% or more when diffuse functions are missing, except with the rather extended cc-pVTZ basis set. Qualitatively, the effects are similar for NMBA, whereas the underestimations are slightly smaller. These results also demonstrate that (i) adding *d* polarization functions increases the average polarizability by about 2–3%, whereas (ii) the *p* polarization functions on the hydrogen atoms have negligible effects and that (iii) going from double-ζ to triple-ζ basis set has a negligible impact if the basis set already contains diffuse functions, while (iv) in the other cases, the effect is at most an increase by 2–3%. This analysis is valid for both the static and dynamic polarizability values.

The situation is partly different for the first hyperpolarizability because the second-order HRS response is dominated by a few tensor

TABLE II

Basis set effects on the CPHF static polarizabilities ($\bar{\alpha}$), first hyperpolarizabilities (β_{HRS}), and depolarization ratios (DR) of POA and NMBA.

	POA			NMBA		
	$\bar{\alpha}$	β_{HRS}	DR	$\bar{\alpha}$	β_{HRS}	DR
6-31G	84.36	278.4	3.16	171.65	905.9	4.23
6-31G*	87.30	249.8	3.14	175.52	867.7	4.32
6-31G**	87.54	249.4	3.15	176.54	867.9	4.31
6-31+G	96.32	305.8	3.05	192.97	989.1	4.10
6-31+G*	98.83	278.9	3.06	196.83	954.4	4.18
6-311G*	89.97	259.2	3.12	183.73	889.7	4.23
6-311G**	90.40	260.7	3.12	184.89	887.1	4.22
6-311+G*	99.05	284.9	3.05	198.20	989.7	4.20
6-311+G**	99.41	286.7	3.06	199.28	986.6	4.19
cc-pVDZ	88.20	250.3	3.11	181.45	860.6	4.23
cc-pVTZ	97.13	257.6	3.10	195.61	911.3	4.24
aug-cc-pVDZ	104.55	272.8	3.10	207.10	988.9	4.25
aug-cc-pVTZ	104.99	273.7	3.10	—	—	—

The $\bar{\alpha}$ and β_{HRS} values are given in atomic units (a.u.).

components. Thus, considering the POA molecule, (i) the 6-31G basis set provides a very good estimate of the aug-cc-pVTZ values, (ii) the agreement gets worse if adding only *d* polarization functions (underestimation by 10%) or if adding only diffuse functions (overestimation by 12%), (iii) a good match with the reference aug-cc-pVTZ values is retrieved with a balanced basis set containing both (6-31+G*: overestimation of less than 2%), (iv) if going from double-ζ to triple-ζ basis set, the HRS first hyperpolarizability increases by 10–15 a.u., which means that the 6-311+G** basis set overestimates the aug-cc-pVDZ value by 5%. In the case of NMBA, the variations in β_{HRS} upon adding polarization, diffuse, or valence functions in the basis set are similar, but the agreement with the reference values is partly different. Therefore, although the 6-31+G* basis set reproduces the aug-cc-pVDZ result within 4.4%, this underestimation is reduced by a factor of about 7 when using the 6-311+G* basis set. Moreover, for NMBA, the 6-31G value is off by 11% and adding only diffuse functions does not lead to an overestimation. These results contrast with those on small molecules [28], including recent CCSD results by Hammond and Kowalski [29] where accurate first hyperpolarizabilities for water, acetonitrile, and chloroform are shown to require the use of basis sets as large as d-aug-cc-pVTZ and d-aug-cc-pV5Z and where Pople basis sets perform often poorly.

The basis set effects on the depolarization ratios are negligible. Concluding this paragraph, the 6-31+G* and 6-311+G* basis sets constitute a good compromise between accuracy and computational costs for evaluating $\overline{\alpha}$, β_{HRS}, and the depolarization ratios of such D/A π-conjugated systems.

3.2. FREQUENCY DISPERSION EFFECTS

Figure 1 describes the variations of the first hyperpolarizability of POA and NMBA as a function of the frequency of excitation in parallel with the variations of the depolarization ratio. In the 0.0–0.1 a.u. frequency range (corresponding to the wavelength range of ∞–456 nm), the β_{HRS} versus ω curve for POA presents two asymptotes, corresponding to the halves of the first excitation energies. In the same range, the depolarization ratio displays only one large variation. Indeed, DR amounts to roughly 3.0 in the low frequency region, increases with the frequency up to a value close to 7.0 and then strongly decreases to attain values between 0.5 and 1.0 in the 456–506 nm range. These variations originate from the types of tensor components, which dominate the second-order response. Indeed, the β_{xxx} component dominates the response at small frequencies up to about $\hbar\omega = 0.9$ a.u., then other components become dominant, including in-plane off-diagonal tensor components. These results were obtained taking into account the effects of the solvent within the PCM scheme, but similar evolutions of β_{HRS} and DR with ω are observed when considering isolated molecules. A different behavior is observed for β_{HRS} and DR of NMBA in that wavelength range. Indeed, the first hyperpolarizability presents an asymptote around $\lambda = 591$ nm, whereas DR changes drastically around $\lambda = 485$ nm. The DR value is larger in NMBA than in POA and is close to the value of 5, typical of linear D-π-A dipolar compounds. This phenomenon results from the larger extent of π-conjugation, and, at the tensor level, it is associated with a strongly dominant β_{xxx} value. It shows that the depolarization ratio can strongly deviate from the ideal values characteristics of the shape of the NLOphore and therefore that it is highly sensitive to the frequency when the electromagnetic excitation is in resonance with the electronic excited states. Improved characterization of this frequency dispersion effects would require including vibronic effects [30].

3.3. ELECTRON CORRELATION EFFECTS

Electron correlation effects were addressed by comparing the CPHF results to the properties evaluated at the MP2 level using the FF approach. As the FF procedure also provides the HF results, it was possible to check that the numerical differentiation procedure combined with the Romberg scheme attains an accuracy of about 0.01–0.1 and 0.1–1 a.u. for the average polarizability and HRS first hyperpolarizability, respectively. MP2 calculations were carried out for POA, using a large range of atomic basis set as well as, to a lower extent, for NMBA. The results are presented under the form of a graph displaying the ratios between the MP2 and HF values (see Fig. 2) as a function of the basis set. For the average polarizability of POA, (i) the MP2/HF ratio ranges between 1.05 and 1.10, (ii) the largest ratios are observed for basis set containing diffuse functions, (iii) the difference between the ratios for basis sets with and without diffuse basis functions

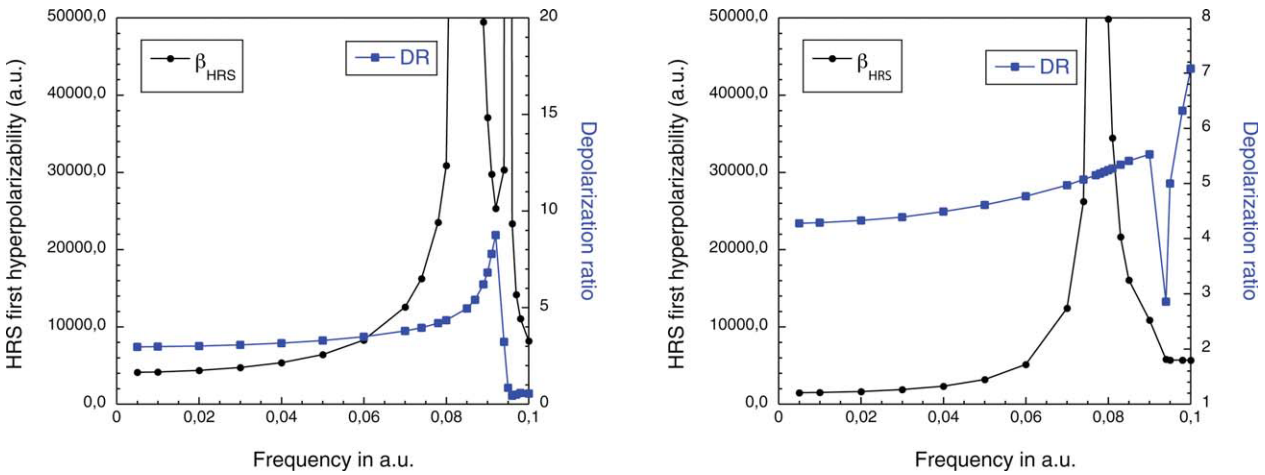

FIGURE 1. Evolution of the HRS first hyperpolarizability and depolarization ratio with the incident light frequency of (left) POA and (right) NMBA. The calculations have been performed at the IEFPCM/TDHF/6-31+G* level of approximation (solvent = acetonitrile). [Color figure can be viewed in the online issue, which is available at wileyonlinelibrary.com.]

amounts roughly to 0.03 as shown by considering the 6-31+G* and aug-cc-pVDZ basis set. In the case of the NMBA compounds, the effects of electron correlation on the average polarizability, as estimated using the MP2 scheme, are even smaller and amount to an increase of $\bar{\alpha}$ by 1–3%.

The effects of electron correlation are much larger for the first hyperpolarizability. As shown in Figure 2, electron correlation leads to an increase of β_{HRS} by 55–70%. Again, larger enhancements are observed for basis sets with diffuse functions. It is also interesting to point out that at the MP2 level the DR of POA ranges from 4.5 to 5.0 as a function of the basis set, whereas it is close to 3.1 at the HF level. Like for the average polarizability, in the case of NMBA, the electron correlation effects on β_{HRS} are much smaller. Using the 6-31G* basis set, the β_{HRS}(MP2)/β_{HRS} (HF) ratio is smaller than 1.2, and it further decreases when adding p polarization functions on the H atoms or a third set of valence functions, or when adding both. On the other hand, when using the 6-31+G* basis set, adding electron correlation at the MP2 level leads to an increase of

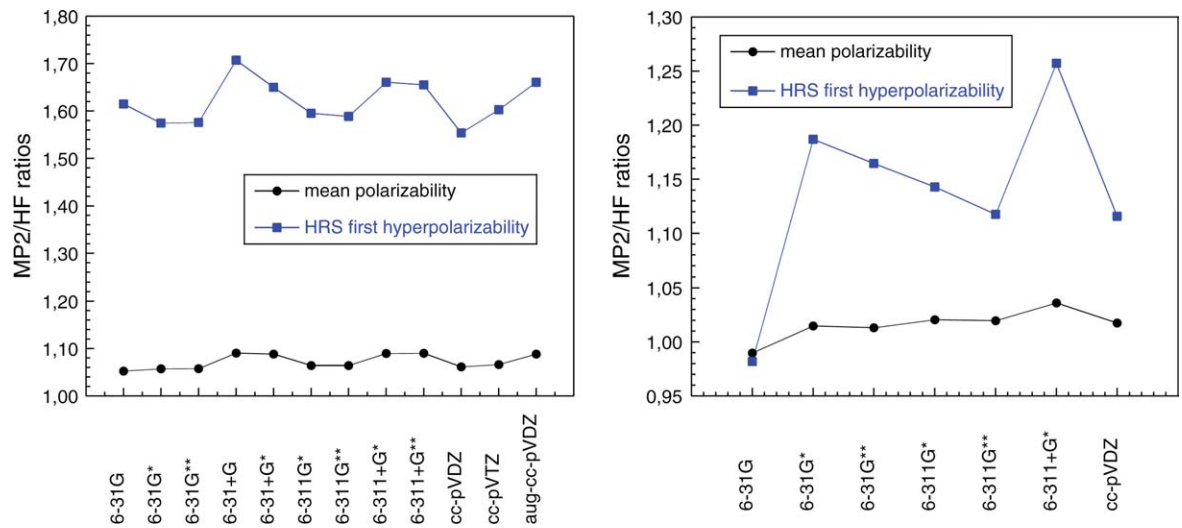

FIGURE 2. Evaluation of the electron correlation effects on the mean polarizability and on the HRS first hyperpolarizability of POA (left) and NMBA (right) estimated by their MP2/HF ratios for different atomic basis sets. [Color figure can be viewed in the online issue, which is available at wileyonlinelibrary.com.]

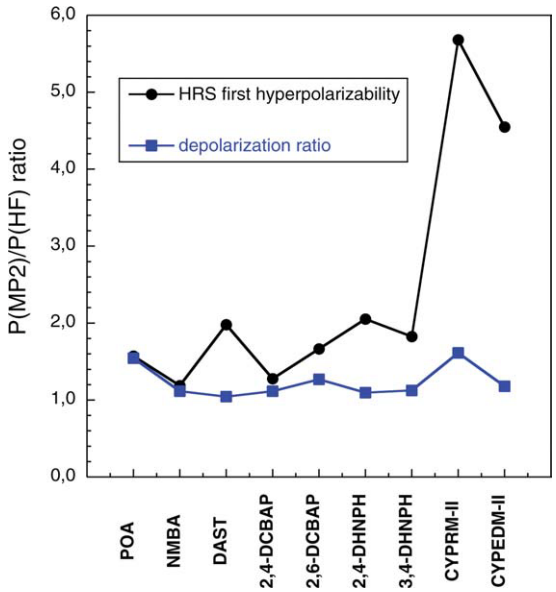

FIGURE 3. Effect of electron correlation, estimated at the MP2/6-31G* level of approximation, on the HRS first hyperpolarizability and depolarization ratio. [Color figure can be viewed in the online issue, which is available at wileyonlinelibrary.com.]

β_{HRS} by 26%. Although these effects are smaller than in the case of POA, their relative amplitudes when inclusion of diffuse, polarization, and/or valence basis functions are similar.

An additional characterization of the electron correlation effects is provided by the investigation of the whole set of compounds at the MP2/6-31G* level of approximation. Figure 3 shows the variations of the $\beta_{HRS}(MP2)/\beta_{HRS}$ (HF) and DR(MP2)/DR(HF) ratios as a function of the nature of the compound. It is interesting to note that the β_{HRS} ratio is close to 5 for CYPRM and CYPEDM, whereas it is often ranging between 1.5 and 2.0. Therefore, the effects of electron correlation might be much different from one compound to another. This statement is also verified for analogous species: $\beta_{HRS}(MP2)/\beta_{HRS}$ (HF) = 1.28 for 2,4-DCBAP but 1.66 for 2,6-DCBAP and $\beta_{HRS}(MP2)/\beta_{HRS}$ (HF) = 2.05 for 2,4-DHNPH but 1.83 for 3,4-DHNPH.

3.4. EFFECTS OF THE SOLVENT WITHIN THE PCM SCHEME AND STRUCTURE–PROPERTY RELATIONSHIPS

Table III lists the $\bar{\alpha}$ and β_{HRS} values as well as the depolarization ratios for the nine molecules calculated at the TDHF/6-311+G* level of approximation with and without accounting for the effects of the solvent within the IEFPCM scheme. Contrasted behaviors are observed. At λ = 1,064 nm, accounting for the solvent results in an increase of the average polarizability by typically 10%, whereas these effects are much larger and much more system dependent for the first hyperpolarizability (see Fig. 4). The solvent effects are further enhanced when considering the static responses because the static dielectric constant of acetonitrile (ε_0 = 36.640) is much larger than its optical analog (ε_∞ = 1.806), leading to larger electronic reorganizations. With the exception of the malononitrile-based species, the DR changes little. The important scattering between the β(acetonitrile)/β(in vacuo) ratios also supports the need to take into account the solvent effects when assessing the NLO potential of chromophores.

Figure 5 demonstrates the difficulty of selecting one β quantity to assess the potential of a molecule for second-order NLO applications. Indeed, though larger β_{HRS} values are generally associated with larger norm of the β vector and larger $\beta_{//}$

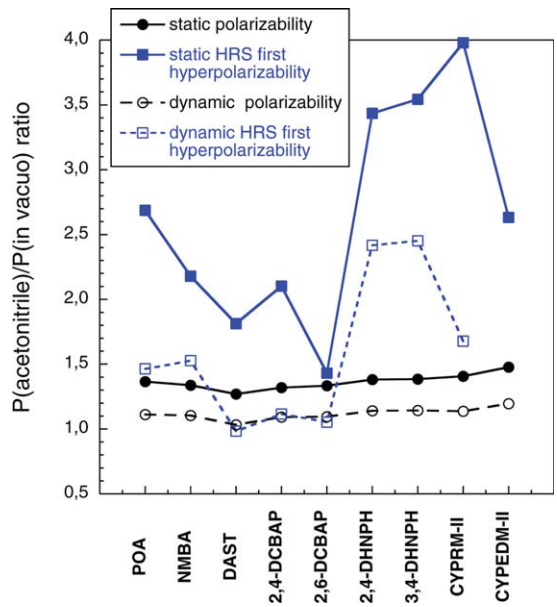

FIGURE 4. Effect of the solvent on the polarizabilities and HRS first hyperpolarizabilities evaluated at the TDHF/6-311+G(d) level of approximation. The dynamic β_{HRS} ratio of CYPEDM has not been included because the value calculated with the IEFPCM scheme is strongly influenced by resonance effects. [Color figure can be viewed in the online issue, which is available at wileyonlinelibrary.com.]

TABLE III

Polarizability, first hyperpolarizability, and depolarization ratio calculated at the TDHF/6–311+G* level of approximation with and without taking into account the effects of the solvent using the IEFPCM scheme.

	Isolated molecules			IEFPCM (acetonitrile)		
	$\overline{\alpha}$	β_{HRS}	DR	$\overline{\alpha}$	β_{HRS}	DR
$\omega = 0$						
POA	99.05	284.9	3.05	135.31	765.5	3.04
NMBA	198.20	989.7	4.20	265.10	2156.8	4.12
DAST	277.08	8447.2	4.65	352.08	15313.2	4.48
2,4-DCBAP	261.53	185.1	2.41	345.08	389.0	3.13
2,6-DCBAP	253.98	265.6	3.01	338.83	380.1	2.30
2,4-DHNPH	207.81	1083.5	4.71	287.12	3722.6	4.61
3,4-DHNPH	209.48	1176.9	4.54	290.17	4170.3	4.45
CYPRM	535.73	3142.6	2.73	753.77	12507.6	2.42
CYPEDM	620.68	7163.8	4.12	917.26	18856.8	3.27
$\omega = 0.042824$ au						
POA	100.55	383.2	3.28	111.79	561.0	3.20
NMBA	202.72	1651.3	4.45	224.03	2522.0	4.52
DAST	296.02	20642.4	4.87	305.64	20314.4	4.81
2,4-DCBAP	265.92	277.8	2.34	290.21	309.9	2.04
2,6-DCBAP	257.73	399.9	3.26	282.34	420.9	2.77
2,4-DHNPH	212.85	1596.0	4.86	243.00	3857.0	4.84
3,4-DHNPH	214.78	1734.5	4.68	245.66	4253.6	4.75
CYPRM	573.85	11320.4	3.59	653.10	18994.2	2.22
CYPEDM	688.49	53263.3	4.94	823.53	824153.7	3.66

For CYPRM and CYPEDM, only the most stable conformer (I) was considered.

values, there are also exceptions and deviations, which result for the presence of several nonnegligible β tensor components in addition to the diagonal component along the longitudinal or charge transfer axis ($\beta_{CT} = \beta_L = \beta_{zzz}$). These are linked to the angle θ between the dipole moment and first hyperpolarizability vectors that influences the $\beta_{//}$ value (Eq. 7). Thus, considering both the static and dynamic results (Table IV), $\beta_{//}$ of POA is particularly small, whereas its intrinsic β response—estimated here by the norm of β or the HRS response—is larger than in the two DCBAP compounds. The two DCBAP isomers differ only by the position (4 or 6) of one chlorine atom, but this has a nonnegligible impact on the molecular properties. Indeed, when the Cl atom is in position 4 (in *para* position of the linker), (i) the dipole moment is larger, (ii) the norm of β increases, (iii) the depolarization ratio is larger (3.13 versus 2.30), (iv) the θ angle is much different from 90° and therefore the $\beta_{//}$ is more than three times larger, but (v) the β_{HRS} responses are similar. At λ = 1,064 nm, ||beta|| and β_{HRS}—as well as the depolarization ratio—of the 2,6-DCBAP compound get larger than in 2,4-DCBAP, whereas the $\beta_{//}$ values of both isomers reduce considerably because θ gets closer to $\pi/2$.

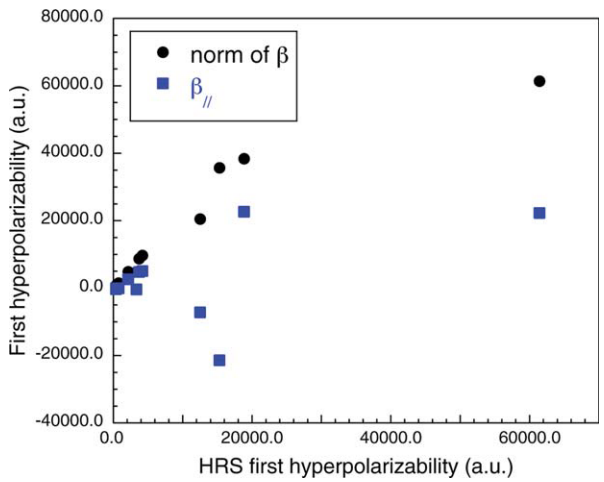

FIGURE 5. Relationship between β_{HRS}, the norm of the β vector and $\beta_{//}$. The calculations were performed at the CPHF/6-311+G* level of approximation. [Color figure can be viewed in the online issue, which is available at wileyonlinelibrary.com.]

TABLE IV

Norms of the μ and β vectors, angle (θ, in degrees) between them as well as $\beta_{//}$ and β_{HRS} values calculated at the TDHF/6–311+G* level of approximation taking into account the effects of the solvent using the IEFPCM scheme.

	$\|\|\mu\|\|$	$\|\|\beta\|\|$	θ	$\beta_{//}$	β_{HRS}
			$\omega = 0.0$ a.u.		
POA	2.70	1494.3	91.7	−26.7	765.5
NMBA	2.94	4880.7	26.9	2610.9	2156.8
DAST	5.08[a]	35698.1	179.0	−21415.6[a]	15313.2
2,4-DCBAP	4.07	772.7	132.2	−311.6	389.0
2,6-DCBAP	3.28	591.4	105.7	−95.7	380.1
2,4-DHNPH	4.25	8765.2	24.3	4794.1	3722.6
3,4-DHNPH	4.85	9699.6	29.2	5079.4	4170.3
CYPRM-I	14.27	20473.2	125.9	−7202.0	12507.6
CYPRM-II	11.79	4832.3	98.1	−408.5	3349.3
CYPEDM-I	13.15	38392.2	10.3	22664.4	18856.8
CYPEDM-II	15.82	61415.5	52.8	22302.4	30819.4
			$\omega = 0.042824$ a.u.		
POA		1126.3	90.7	−8.8	561.0
NMBA		5875.4	26.0	3168.3	2522.0
DAST		48224.3	179.7	−28934.1	20314.4
2,4-DCBAP		408.2	121.5	−128.0	309.9
2,6-DCBAP		774.0	97.7	−62.0	420.9
2,4-DHNPH		9196.6	25.1	4998.7	3857.0
3,4-DHNPH		10082.7	29.5	5263.2	4253.6
CYPRM-I		30517.9	102.8	−4061.9	18994.2
CYPRM-II		15891.0	145.9	−7899.4	6673.6
CYPEDM-I		NR[b]	27.5	NR	NR
CYPEDM-II		NR	4.4	NR	NR

All μ and β values are given in a.u.

[a] The origin of the Cartesian axes coincides with the molecule center of mass (the charge of the molecule is nonzero).

[b] Near resonance (NR) conditions.

With respect to the DCBAP compounds, the first hyperpolarizabilities of the two DHNPH isomers are, at least, one order of magnitude larger, though they are of similar size. The θ angles are rather small ($\theta < \pi/6$) and change little when going from the static to the dynamic quantities. This can be attributed to the dipolar character of the DHNPH isomers as substantiated by depolarization ratios close to 5 (Table III). The static first hyperpolarizabilities of NMBA are roughly a factor of 2 smaller than those of the DCBAP isomers, and the dipolar character of NMBA is less pronounced (smaller DR value). When turning to the dynamic β values at 1,064 nm, the difference between NMBA and DCBAP gets slightly smaller. This smaller NLO potential of NMBA with respect to DCBAP can be attributed to the combination of the size of the conjugated linker and the strength of the D/A groups. Indeed, NMBA contains only a strong acceptor group (NO_2). On the other hand, the situation is different in DAST, which contains a pair of strong D/A substituents, while it is of the same size as NMBA. Indeed, in DAST, the first hyperpolarizabilities are four to five times larger than in the two DCBAP isomers and about one order of magnitude larger than in NMBA. These large responses are associated with a strong dipolar character (DR close to 5) and an antiparallel alignment of the μ and β vectors ($\theta \sim \pi$). This analysis further highlights the impact of the θ angle on the EFISHG response and, in a number of cases, its sensitivity to the type of calculation (with or without solvent effects, static or dynamic responses). In these cases of high sensitivity, θ is close to $\pm\pi/2$ and small variations lead to large changes of $\beta_{//}$. This suggests that a

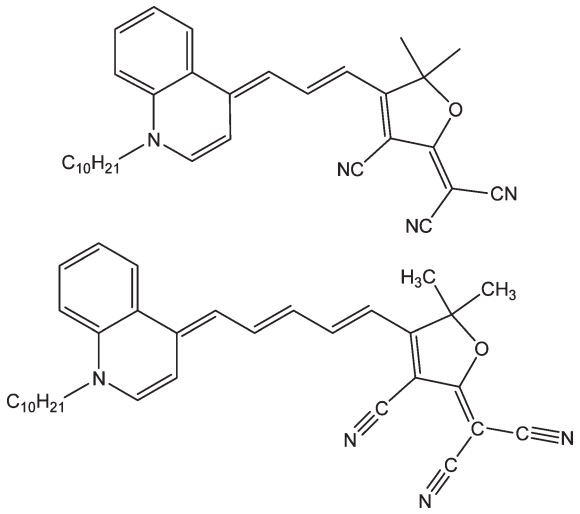

SCHEME 2. Sketch of the alternative (stable) conformations of (top) 2-{3-cyano-4-[3-(1-decyl-1,4-dihydroquinolin-4-ylidene)prop-1-enyl]-5,5-dimethyl-2,5-dihydrofuran-2-ylidene}malononitrile (CYPRM) and (bottom) 2-{3-cyano-4-[5-(1-decyl-1,4-dihydroquinolin-4-ylidene)-penta-1,3-dienyl]-5,5-dimethyl-2,5-dihydrofuran-2-ylidene}malononitrile (CYPEDM).

reliable characterization of the second-order NLO response—or of its potential in view of applications in the solid state—should avoid this quantity and concentrate on the HRS response. Note that analogous angle effects have also been highlighted when interpreting VCD spectra of chiral species, leading to the definition of robust modes [31].

Substantial second-order NLO responses are also achieved with the CYPRM and CYPEDM compounds (Tables III and IV), which exhibit the typical β enhancement upon enlarging the conjugated path by one CH=CH unit. However, these compounds display less dipolar character, in particular CYPRM, of which the depolarization ratio is smaller than 2.5. In CYPRM, the angle between the μ and β vectors is also far from 0 or π, which explains the smaller EFISHG responses. When inserting one CH=CH unit in the π-conjugated linker between the donor and the acceptor moieties, the dipolar character increases and the μ and β vectors get almost aligned. In that case, the β responses are larger than in DAST, though the size of the compound is much larger. The results at 1,064 nm go in the same direction, though the CYPEDM responses are impacted by near resonance effects.

CYPRM and CYPEDM have been further characterized by considering a second stable conformer (Scheme 2). For both compounds, the most stable conformer (Scheme 1) is characterized by an all trans-transoïd conformation of the linker, whereas the second conformer presents one trans-cisoïd moiety. Considering the B3LYP/6-311G(d)-optimized geometries, the HF/6-311+G*/IEFPCM energy of the second conformer is higher by 1.65 and 3.10 kcal/mol for CYPRM and CYPEDM, respectively. As already pointed out in several investigations [32], conformational changes are associated with substantial modifications of the NLO properties, encompassing large changes of DR, θ, β_{HRS}, $\|\beta\|$, and $\beta_{//}$. This is verified here.

Among all compounds, DAST, CYPRM, and CYPEDM present the largest first hyperpolarizabilities and therefore the largest potential in view of preparing materials with large $\chi^{(2)}$ responses. This conclusion is substantiated by the MP2/6-31G* calculations of the static first hyperpolarizabilities (Table V). Finally, considering Eq. (1), the best estimate for the $\beta_{HRS}(-2\omega;\ \omega,\ \omega)$ value (λ = 1,064 nm) of the isolated species amounts to 41, 64, and 242 $\times$ 10^3 a.u. for DAST, CYPRM, and CYPEDM, respectively. When including the solvent effects, the corresponding values for DAST and CYPRM are 40 and 108 $\times$ 10^3 a.u. With the exception of the two DCBAP compounds, which present small second-order NLO responses, all DR ratios estimated at the MP2 level are close to the dipolar value of 5.

TABLE V

Norms of the μ as well as $\beta_{//}$, β_{HRS}, and DR values calculated at the MP2/6–31G* level of approximation.

	$\|\|\mu\|\|$	$\beta_{//}$	β_{HRS}	DR
POA	1.82	19	393	4.85
NMBA	2.01	1394	1030	4.82
DAST	3.42[a]	−22967[a]	15981	4.86
2,4-DCBAP	2.47	−7	253	2.44
2,6-DCBAP	1.82	−20	481	3.58
2,4-DHNPH	2.36	2554	1982	5.27
3,4-DHNPH	2.96	2378	1860	5.17
CYPRM	8.38	23427	16386	5.29
CYPEDM	7.53	46217	33718	5.01

All μ and β values are given in a.u.

[a] The origin of the Cartesian axes coincides with the molecule center of mass (the charge of the molecule is nonzero).

4. Conclusions and Outlook

The first hyperpolarizabilities (and, to a lower extent, also the polarizability) of nine chromophores have been calculated ab initio to assess the effects of basis sets, of electron correlation (at the MP2 level), of frequency dispersion, and of the solvent within the polarizable continuum model, as well as to address structure–property relationships. These chromophores have been chosen because they have recently been synthesized and because crystals have been grown in view to achieve large second-order NLO susceptibilities. The main observations are (i) a confirmation that moderate-size basis sets like 6-31+G* and 6-311+G* are enough to provide accurate estimates of the polarizabilities and first hyperpolarizabilities for these systems build from the combination of π-conjugated linkers with D/A moieties, (ii) the specific behavior of the HRS first hyperpolarizability and of its depolarization ratio as a function of the incident light frequency, (iii) the fact that electron correlation effects are not only large but also strongly compound dependent, and (iv) the similar role played by the solvent, which enhances the first hyperpolarizabilities by amplitudes depending on the nature of the compound.

Supporting Information: The B3LYP/6-311G(d) optimized geometries of the different compounds.

ACKNOWLEDGMENT

The calculations have been performed on the Interuniversity Scientific Computing Facility (ISCF), installed at the FUNDP.

References

1. Shi, Y. Q.; Zhang, C.; Zhang, H.; Bechtel, J. H.; Dalton, L. R.; Robinson, B. H.; Steier, W. H. Science 2000, 288, 119.
2. Ma, H.; Jen, A. K. Y.; Dalton, L. R. Adv Mater Weinheim Ger 2002, 14, 1339.
3. Schneider, A.; Neis, M.; Stillhart, M.; Ruiz, B.; Khan, R. U. A.; Günter, P. J Opt Soc Am B 2006, 23, 1822.
4. (a) Ruiz Delgado, M. C.; Casado, J.; Hernandez, V.; Lopez Navarrete, J. T.; Orduna, J.; Villacampa, B.; Alicante, R.; Raimundo, J. M.; Blanchard, P.; Roncali, J. J Phys Chem C 2008, 112, 3109; (b) Wang, Y.; Frattarelli, D. L.; Facchetti, A.; Cariati, E.; Tordin, E.; Ugo, R.; Zuccaccia, C.; Macchioni, A.; Wegener, S. L.; Stern, C. L.; Ratner, M. A.; Marks, T. J. J Phys Chem C 2008, 112, 8005; (d) Corozzi, A.; Mennucci, B.; Cammi, R.; Tomasi, J. J Phys Chem A 2009, 113, 14774; (e) De Meulenaere, E.; Asselberghs, I.; de Wergifosse, M.; Botek, E.; Spaepen, S.; Champagne, B.; Vanderleyden, J.; Clays, K. J Mater Chem 2009, 19, 7514.
5. (a) Gilat, S. L.; Kawaï, S. H.; Lehn, J. M. Chem Eur J 1995, 1, 275; (b) Sliwa, M.; Létard, S.; Malfrant, I.; Nierlich, M.; Lacroix, P. G.; Asahi, T.; Matsuhara, H.; Yu, P.; Nakatani, K. Chem Mater 2005, 17, 4727; (c) Coe, B. J. Acc Chem Res 2006, 39, 383; (d) Plaquet, A.; Guillaume, M.; Champagne, B.; Rougier, L.; Mançois, F.; Rodriguez, V.; Pozzo, J. L.; Ducasse, L.; Castet, F. J Phys Chem C 2008, 112, 5638; (e) Aubert, V.; Guerchais, V.; Ishow, E.; Hoang-Thi, K.; Ledoux, I.; Nakatani, K.; Le Bozec, H. Angew Chem Int Ed 2008, 47, 577; (f) Mançois, F.; Pozzo, J. L.; Adamietz, F.; Rodriguez, V.; Ducasse, L.; Castet, F.; Plaquet, A.; Champagne, B. Chem Eur J 2009, 15, 2560.
6. (a) Botek, E.; Spassova, M.; Champagne, B.; Asselberghs, I.; Persoons, A.; Clays, K. Chem Phys Lett 2005, 412, 274; (b) Botek, E.; Spassova, M.; Champagne, B.; Asselberghs, I.; Persoons, A.; Clays, K. Chem Phys Lett 2006, 417, 282; (c) Bossi, A.; Licandro, E.; Maiorana, S.; Rigamonti, C.; Righetto, S.; Stephenson, G. R.; Spassova, M.; Botek, E.; Champagne, B. J Phys Chem C 2008, 112, 7900.
7. Kanis, D. R.; Ratner, M. A.; Marks, T. J. Chem Rev 1994, 94, 195.
8. Champagne, B.; Kirtman, B. In Handbook of Advanced Electronic and Photonic Materials and Devices; Nalwa, H. S., Ed.; Academic Press: New York, 2001; Vol. 9, Chapter 2, p 63.
9. Suponitsky, K. Y.; Timofeeva, T. V.; Antipin, M. Y. Rus Chem Rev 2006, 75, 457.
10. Keinan, S.; Therien, M. J.; Beratan, D. N.; Yang, W. J Phys Chem A 2008, 112, 12203.
11. (a) Xiao, D.; Bulat, F. A.; Yang, W.; Beratan, D. N. Nano-Lett 2008, 8, 2814; (b) Chen, W.; Yu, G. T.; Gu, F. L.; Aoki, Y. J Phys Chem C 2009, 113, 8447; (c) Loboda, O.; Zalesny, R.; Avramopoulos, A.; Luis, J. M.; Kirtman, B.; Tagmatarchis, N.; Reis, H.; Papadopoulos, M. G. J Phys Chem A 2009, 113, 1159.
12. (a) Zjang, C.; Dalton, L. R.; Oh, M. C.; Zhang, H.; Steier, W. H. Chem Mater 2001, 13, 3043; (b) Perez-Moreno, J.; Zhao, Y.; Clays, K.; Kuzyk, M. G. Opt Lett 2007, 32, 59.
13. Wu, W.; Wu, D.; Cheng, W.; Zhang, H.; Dai, J. Cryst Growth Des 2007, 7, 2316.
14. Srinivasan, K.; Biravaganesh, R.; Gandhimathi, R.; Ramasamy, P. J Cryst Growth 2002, 236, 381.
15. Ruiz, B.; Jazbinsek, M.; Gunter, P. Cryst Growth & Design 2008, 8, 4174.
16. Sun, Y. X.; Wei, W. X.; Hao, Q. L.; Lu, L.-D.; Wang, X. Spectrochim Acta A 2009, 73, 7721.
17. Kwon, O. P.; Jazbinsek, M.; Seo, J.-In.; Choi, E.-Y.; Yun, H.; Brunner, F. D. J.; Lee, Y. S.; Günter, P. J Chem Phys 2009, 130, 134708.
18. Gainsford, G. J.; Delower, M.; Bhuiyan, H.; Kay, A. J. Acta Cryst C 2008, 64, o616.
19. (a) Canuto, S.; Duch, W.; Geertsen, J.; Muller-Plathe, F.; Oddershede, J.; Scuseria, G. E. Chem Phys Lett 1988, 147, 435; (b) Castro, A.; Canuto, S. Phys Lett A 1993, 176, 105; (c) Canuto, S.; Castro, M. A.; Mukherjee, P. K. Phys Rev A 1994, 49, 3515; (d) Canuto, S. Int J Quantum Chem 1997, 63, 459.
20. (a) Serrano, A.; Canuto, S. Int J Quantum Chem 2002, 87, 275; (b) Serrano, A.; Canuto, S. Int J Quantum Chem 1998, 70, 745; (c) Canuto, S.; Coutinho, K.; Mukherjee, P. K. Adv

Quantum Chem 2005, 48, 141; (d) Coutinho, K.; Canuto, S. In Atoms, Molecules and Clusters in Electric Fields. Theoretical Approaches to the Calculation of Electric Polarizability; Maroulis, G., Ed.; Imperial College Press: London, 2005; p 405.

21. (a) Sekino, H.; Bartlett, R. J. J Chem Phys 1986, 85, 976; (b) Karna, S. P.; Dupuis, M. J Comput Chem 1991, 12, 487.
22. (a) Tomasi, J.; Persico, M. Chem Rev 1994, 94, 2027; (b) Tomasi, J.; Mennucci, B.; Cammi, R. Chem Rev 2005, 105, 2999.
23. (a) Sekino, H.; Bartlett, R. J. Chem Phys Lett 1995, 234, 87; (b) Dalskov, E.; Jensen, H. J. A.; Oddershede, J. Mol Phys 1997, 90, 3; (c) Jacquemin, D.; Champagne, B.; Hättig, C. Chem Phys Lett 2000, 319, 327.
24. Bersohn, R.; Pao, Y. H.; Frisch, H. L. J Chem Phys 1966, 45, 3184.
25. Yang, M.; Champagne, B. J Phys Chem A 2003, 107, 3942.
26. Michl, J., Ed. Chem Rev 1994, 94, 1.
27. Frisch, M. J.; Trucks, G. W.; Schlegel, H. B.; Scuseria, G. E.; Robb, M. A.; Cheeseman, J. R.; Montgomery, J. A., Jr.; Vreven, T.; Kudin, K. N.; Burant, J. C.; Millam, J. M.; Iyengar, S. S.; Tomasi, J.; Barone, V.; Mennucci, B.; Cossi, M.; Scalmani, G.; Rega, N.; Petersson, G. A.; Nakatsuji, H.; Hada, M.; Ehara, M.; Toyota, K.; Fukuda, R.; Hasegawa, J.; Ishida, M.; Nakajima, T.; Honda, Y.; Kitao, O.; Nakai, H.; Klene, M.; Li, X.; Knox, J. E.; Hratchian, H. P.; Cross, J. B.; Adamo, C.; Jaramillo, J.; Gomperts, R.; Stratmann, R. E.; Yazyev, O.; Austin, A. J.; Cammi, R.; Pomelli, C.; Ochterski, J. W.; Ayala, P. Y.; Morokuma, K.; Voth, G. A.; Salvador, P.; Dannenberg, J. J.; Zakrzewski, V. G.; Dapprich, S.; Daniels, A. D.; Strain, M. C.; Farkas, O.; Malick, D. K.; Rabuck, A. D.; Raghavachari, K.; Foresman, J. B.; Ortiz, J. V.; Cui, Q.; Baboul, A. G.; Clifford, S.; Cioslowski, J.; Stefanov, B. B.; Liu, G.; Liashenko, A.; Piskorz, P.; Komaromi, I.; Martin, R. L.; Fox, D. J.; Keith, T.; Al-Laham, M. A.; Peng, C. Y.; Nanayakkara, A.; Challacombe, M.; Gill, P. M. W.; Johnson, B.; Chen, W.; Wong, M. W.; Gonzalez, C.; Pople, J. A. GAUSSIAN 03 (Revision C. 02); Gaussian Inc.: Wallingford, CT, 2004.
28. (a) Sekino, H.; Bartlett, R. J. J Chem Phys 1993, 98, 3022; (b) Yamada, S.; Nakano, M.; Shigemoto, I.; Kiribayashi, S.; Yamaguchi, K. Chem Phys Lett 1997, 267, 445; (c) Maroulis, G. J Chem Phys 1998, 108, 5432; (d) Kamada, K.; Ueda, M.; Nagao, H.; Tawa, K.; Sugino, T.; Shimizu, Y.; Ohta, K. J Phys Chem A 2000, 104, 4723; (e) Pecul, M.; Pawlowski, F.; Jørgensen, P.; Köhn, A.; Hättig, C. J Chem Phys 2006, 124, 114101; (f) Maroulis, G. J Chem Phys 2008, 129, 044314; (g) O'Neill, D. P.; Kallay, M.; Gauss, J. J Chem Phys 2007, 127, 134109; (h) Baranovska, A.; Sadlej, A. J. J Comput Chem 2010, 31, 552.
29. Hammond, J. R.; Kowalski, K. J Chem Phys 2009, 130, 194108.
30. Campo, J.; Wenseleers, W.; Goovaerts, E.; Szablewski, M.; Cross, G. H. J Phys Chem C 2008, 112, 287.
31. Nicu, V. P.; Baerends, E. J. Phys Chem Chem Phys 2009, 11, 6107.
32. (a) Mançois, F.; Sanguinet, L.; Pozzo, J. L.; Guillaume, M.; Champagne, B.; Rodriguez, V.; Adamietz, F.; Ducasse, L.; Castet, F. J Phys Chem B 2007, 111, 9795; (b) Chafin, A. P.; Lindsay, G. A. J Phys Chem C 2008, 112, 7829.